Inorganic Chemistry

Article

pubs.acs.org/IC

Self-Decelerating Relaxation of the Light-Induced Spin States in Molecular Magnets $Cu(hfac)_2L^R$ Studied by Electron Paramagnetic Resonance

Matvey V. Fedin,* Ksenia Yu. Maryunina, Renad Z. Sagdeev, Victor I. Ovcharenko, and Elena G. Bagryanskaya

International Tomography Center SB RAS, Institutskaya str. 3a, 630090, Novosibirsk, Russia

Supporting Information

ABSTRACT: Molecular magnets $Cu(hfac)_2L^R$ (hfac = hexafluoroacetylacetonate) called "breathing crystals" exhibit thermally and light-induced magnetic anomalies very similar to iron(II) spin-crossover compounds. They are physically different systems, because the spin-state switching occurs in exchange-coupled nitroxide−copper(II)−nitroxide clusters, in contrast to classical spin crossover in d^4−d^7 transition ions. Despite this difference, numerous similarities in physical behavior of these two types of compounds have been observed, including light-induced excited spin-state trapping (LIESST) phenomenon recently found in the $Cu(hfac)_2L^R$ family. Similar to iron(II) spin-crossover compounds, the excited spin state in breathing crystals relaxes to the ground state on the time scale of hours at cryogenic temperatures. In this work, we investigate this slow relaxation in a series of breathing crystals using electron paramagnetic resonance (EPR). Three selected compounds represent the cases of relatively strong or weak cooperativity and different temperature of thermal spin transition. They all were studied in a neat magnetically concentrated form; however, sigmoidal self-accelerating relaxation was not observed. On the contrary, the relaxation shows pronounced self-decelerating character for all studied compounds. Relaxation curves and their temperature dependence could be fitted assuming a tunneling process and broad distribution of effective activation energies in these 1D materials. A number of additional experimental and theoretical arguments support the distribution-based model. Because self-decelerating relaxation behavior was also found in 1D polymeric iron(II) spin-crossover compounds previously, we compared general relaxation trends and mechanisms in these two types of systems. Both similarities and differences of copper−nitroxide-based breathing crystals as compared to iron(II) spin-crossover compounds make future research of light-induced phenomena in these new types of spin-crossover-like systems topical in the field of molecule-based magnetic switches.

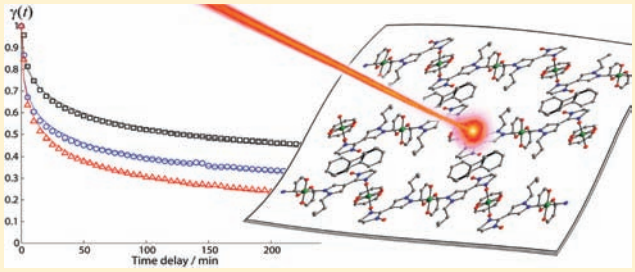

INTRODUCTION

Design of molecule-based magnetic switches operated by external stimuli attracted significant attention during last two decades.[1−7] Along with the fundamental importance, the interest to such systems is stimulated by potential applications in nanotechnology. Most of the studies carried so far were focused on spin-crossover and valence tautomeric transition-metal complexes. Spin multiplicity of the ground state of the transition-metal ion in these compounds can be changed between high-spin (HS) and low-spin (LS) states by temperature, light, pressure, and other external factors. Most abundantly, the iron(II) spin-crossover compounds were studied up to date.

Recently, a new family of compounds, exhibiting effects quite similar to the spin crossover but of different origin, was found and studied.[8−21] These complexes have a polymeric chain structure based on copper(II) hexafluoroacetyl acetonates $[Cu(hfac)_2]$ and pyrozolyl-substituted nitronyl nitroxide radicals (L^R). The structure and magnetic susceptibility of complexes $Cu(hfac)_2L^R$ reversibly changes with temperature, in many respects resembling the manifestation of spin crossover. In most of the compounds $Cu(hfac)_2L^R$, the observed magnetic anomalies occur in the exchange-coupled spin triads nitroxide−copper(II)−nitroxide. Although the copper(II) ion cannot experience spin crossover because of its d^9 electronic configuration, the exchange-coupled three-spin cluster can change its spin configuration between weakly coupled and strongly coupled spin states (WS and SS states, respectively). Usually, the WS state is found at high temperatures, where the nitroxide spins occupy axial positions with respect to the copper atom and the exchange coupling is weak. On lowering the temperature, structural rearrangements occur in CuO_6 octahedra, leading to the shortening of distances between copper and nitroxides and conversion of nitroxides to the equatorial positions. In this case, the exchange coupling becomes strong antiferromagnetic, and the spin triad converts to the SS state. These structural rearrangements and spin

Received: October 17, 2011
Published: December 14, 2011

   dx.doi.org/10.1021/ic202248v | Inorg. Chem. 2012, 51, 709−717

transitions between SS and WS states have been detected by X-ray, magnetometry, electron paramagnetic resonance (EPR), and other spectroscopic techniques.[8−21] Because of the large and reversible variation of unit cell volume (up to ca. 13%) during thermal spin transitions, the compounds $Cu(hfac)_2L^R$ have also been called "breathing crystals".

Interesting thermally induced structural and magnetic anomalies have also been observed in several compounds based on copper(II) and/or nitroxides, including manifestations of unique thermochromism and magnetic phase transition,[22] spin-transition-like behavior in a nitroxide−copper(II)−nitroxide spin triad,[23] magnetic bistability and thermochromism in a molecular copper(II) chain,[24] etc.[25−28]

Apart from thermal spin transition, recently, the light-induced phenomena have been found in breathing crystals as well.[21] Light-induced spin-state switching is well-known in iron(II) spin-crossover compounds. It was found that for many complexes, the light-induced excited spin state is metastable at low (cryogenic) temperatures on the time scale of hours and days. This phenomenon has been called light-induced excited spin-state trapping (LIESST) and has attracted significant attention during the last several decades.[3−7,29−34] The light-induced HS → LS relaxation has been studied in detail.[35] In particular, it was found that the low-temperature relaxation is a quantum-tunneling process with the thermally activated region at elevated temperatures. Depending on the compound and its form (neat vs magnetically diluted, embedded into the polymer matrices, etc.), a different character of relaxation has been observed. Generally, it is expected that in magnetically diluted systems with weak cooperative interactions, the relaxation is purely monoexponential. However, for systems with high cooperativity, typically compounds in neat form, the relaxation was often found to have the self-accelerating character where the excited-state concentration dependence on time has a sigmoidal shape. The third type of the observed dependence is, the other way around, self-decelerating. As was originally proposed by Hauser et al., this relaxation character is caused by a distribution of relaxation rates in spin-crossover centers.[35,36] In fact, a relatively narrow distribution in the activation energy barrier or zero-point energy difference can lead to significant distribution in relaxation rates and, as a result, a self-decelerating relaxation curve.

The first study of LIESST-like phenomenon in breathing crystals has sketched the main trends of photoswitching and relaxation.[21] Interestingly, the relaxation was found to be fast in the beginning but nearly reaching a plateau in a few hours, which can be explained by two contributions or, alternatively, by self-deceleration. In the present paper, we study this slow self-decelerating relaxation in a series of breathing crystals using EPR. We have developed the approach for relaxation measurements, studied the relaxation depending on temperature and the preparation history, and compared general trends for three selected compounds showing different magnetic behaviors. Complex analysis of all collected data and theoretical modeling allowed us to propose the reasons for self-deceleration and describe the relaxation behavior observed in breathing crystals.

CHOICE OF SYSTEMS AND EXPERIMENTAL DETAILS

We selected three representative compounds of the "breathing crystals" family for the study of light-induced spin-state relaxation: $Cu(hfac)_2L^{Pr}$ (**I**), $Cu(hfac)_2L^{Bu}\cdot C_3H_7-C_5H_6$ (**II**), and $Cu(hfac)_2L^{Bu}\cdot mC_8H_{10}$ (**III**). The syntheses of **I**−**III** and their structural and magnetic properties were described in detail previously.[8,11] The magnetic susceptibility data for these compounds are shown in Figure 1b.[8,11] Compound **I**, which

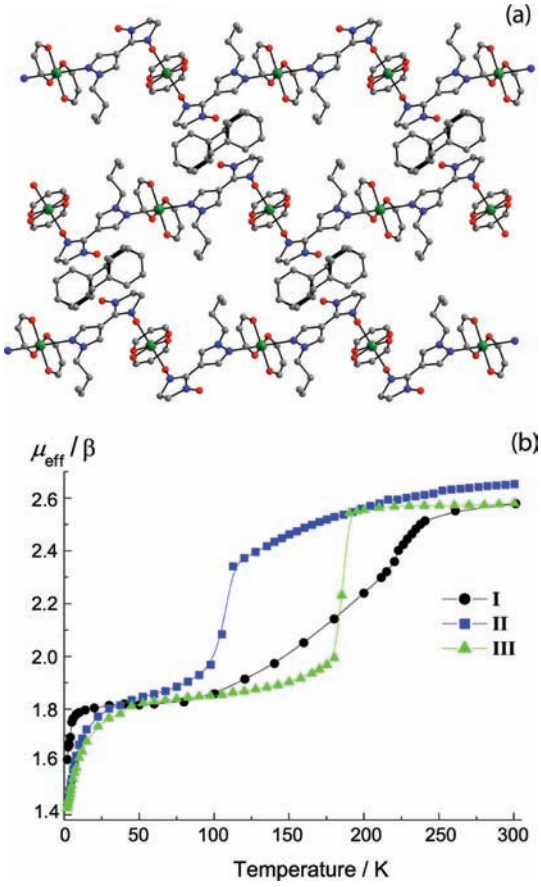

Figure 1. (a) Polymer-chain structure of compound **II**. Propylbenzene molecules ($C_3H_7-C_5H_6$) are disordered. (b) Temperature dependence of the effective magnetic moment of the compounds **I**−**III** (measured previously; see refs 8 and 11).

was also used in our first LIESST experiments, exhibits a gradual spin transition occurring between $T \sim 100$ and 300 K that implies a relatively low degree of cooperativity. Two other compounds represent cases of relatively strong cooperativity and exhibit abrupt spin transitions at $T \sim 105$ K (**II**) and $T \sim 185$ K (**III**) that are close to the minimum and maximum temperatures of abrupt spin transitions in breathing crystals synthesized so far.[8−11]

EPR measurements were carried out in continuous-wave (CW) mode using the commercial X/Q-band (9/34 GHz) EPR spectrometer Bruker Elexsys E580 equipped by an Oxford Instruments temperature control system (T = 4−300 K). For sample preparation, we used the same approach as developed by us in ref 21. The compounds show very intense absorption in UV−vis near-IR regions with the extinction coefficients of up to a few thousands M^{-1} cm^{-1} at 400−600 nm.[21] To make the illumination efficient, crystals were grinded, mixed with an excess of glass-forming liquid (glycerol) to form a suspension, and then frozen at cryogenic temperatures. In situ illumination was done using a LOTIS-TII Nd:YAG laser and OPO system. Pulse illumination has been carried out at 10 Hz with 1−2 mJ per pulse at a wavelength of 900 nm. The typical duration of

dx.doi.org/10.1021/ic202248v | Inorg. Chem. 2012, 51, 709−717

illumination was 5−7 min. After this time, no significant further change of the EPR spectra was observed, meaning that the conversion depth close to the maximum for all spin triads accessible by light was achieved. In a few experiments (Figure 5) where the conversion depth vs time was measured, the sample was illuminated for up to 40 min with the smaller laser light intensity <1 mJ per pulse. The EasySpin toolbox was used for simulation of EPR spectra shown in Figure 2a−c.[37]

SPECTROSCOPIC APPROACH

Investigation of slow relaxation of the light-induced spin states using EPR requires two experimental demands to be overcome. First, the powder EPR spectra of one-spin copper ions and spin triads in WS and SS states significantly overlap.[11−14] In principle, these signals can be partly resolved by going to the higher mw frequencies (e.g., from 9 to 34 GHz), but then, a second complication appears. Recording slow-relaxing spectra requires very high instrumental stability over several hours. We have found that the stability at the X-band is much higher than at the Q-band for the spectrometer used.

Fortunately, a convenient solution was found by subtraction of a dark spectrum (spectrum before light illumination) from spectra collected during relaxation of the system to the ground state. The EPR spectrum before illumination can be written as

$$S_{\mathrm{dark}} = S_{\mathrm{Cu}} + S_{\mathrm{SS}} + S_{\mathrm{baseline}} \quad (1)$$

where S_{Cu} is the spectrum of an one-spin unit containing magnetically isolated copper(II) ion, S_{SS} is the spectrum of the spin triad in the SS state (ground state at low temperatures $T <$ 70 K for all studied compounds), and S_{baseline} contains all other spectra that do not change under light illumination, including resonator baseline, admixtures of crystals dissolved by glycerol during the sample preparation procedure, and crystals in the volume that is not reached by light.

Light illumination converts the fraction γ of spin triads from the SS to the WS state ($0 \le \gamma \le 1$) and, following relaxation, leads to the reverse conversion from WS to SS state, so that introducing $\gamma = \gamma(t)$, we find

$$S_{\mathrm{light}}(t) = S_{\mathrm{Cu}} + \gamma(t)\cdot S_{\mathrm{WS}} + [1 - \gamma(t)]\cdot S_{\mathrm{SS}} + S_{\mathrm{baseline}} \quad (2)$$

where S_{WS} is the spectrum of spin triad in the light-induced WS state. Subtracting eq 1 from eq 2, we obtain the difference spectrum

$$S_{\mathrm{diff}}(t) = S_{\mathrm{light}}(t) - S_{\mathrm{dark}} = \gamma(t)\cdot(S_{\mathrm{WS}} - S_{\mathrm{SS}}) \quad (3)$$

The first advantage of this approach is that the difference spectrum $S_{\mathrm{diff}}(t)$ is free from all light-independent contributions. Second, its shape is time-independent being described by $(S_{\mathrm{WS}} - S_{\mathrm{SS}})$, and its amplitude is proportional to the fraction of spin triads in WS state $\gamma(t)$. Therefore, $\gamma(t)$ can conveniently be measured by monitoring the amplitude of $S_{\mathrm{diff}}(t)$ in the experiment. Note that using this approach does not require individual signals of WS and SS states to be resolved and therefore can be implemented at the X-band, where the stability and other experimental conditions have been found superior as compared to the Q-band used previously.[21]

The developed approach and typically obtained spectra are illustrated in Figure 2. Figure 2a shows calculated individual EPR spectra of magnetically isolated copper ions (S_{Cu}) and spin triads in SS and WS states (S_{SS} and S_{WS}, eqs 1 and 2) that constitute the experimentally observed spectra. Figure 2b shows the calculated spectra before (S_{dark}) and after (S_{light}) illumination, and Figure 2c shows the difference spectrum S_{diff} of eq 3 and illustrates its evolution in time. Finally, Figure 2d shows the experimentally obtained difference spectra $S_{\mathrm{diff}}(t)$ for compound **I** at time delays from 0 to 240 min after illumination. The line shapes of the spectra coincide within experimental accuracy (see the normalized spectra in Figure S1

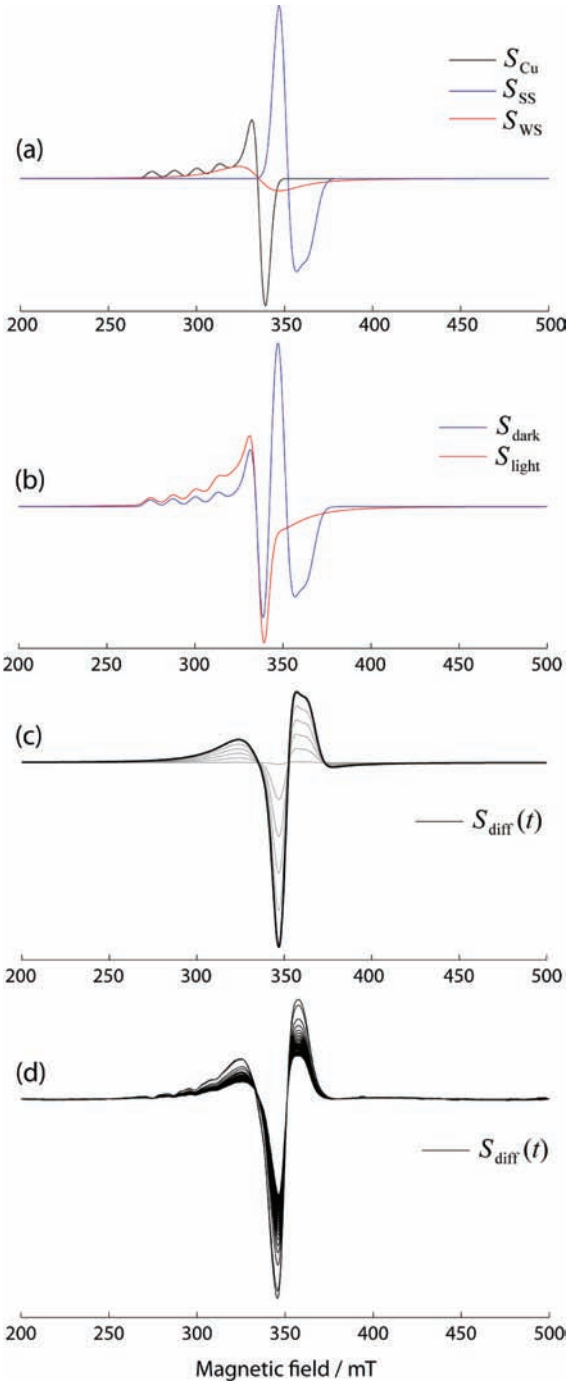

Figure 2. (a) Calculated individual EPR spectra of magnetically isolated copper ion (S_{Cu}) and spin triads in SS and WS states (S_{SS} and S_{WS}). (b) Calculated EPR spectra before (S_{dark}) and after (S_{light}) illumination with light. (c) Difference spectrum S_{diff} calculated for γ = 1 (thick black line) and γ = 0.8, 0.6, 0.4, 0.2, and 0.01 (thin gray lines). (d) Experimentally observed $S_{\mathrm{diff}}(t)$ for compound **I** at time delays 0−240 min after illumination. Colors are indicated in the legends.

dx.doi.org/10.1021/ic202248v | Inorg. Chem. 2012, 51, 709−717

in the Supporting Information), which is a criterion of applicability of this approach, and the corresponding amplitudes characterize the time dependence of the WS fraction $\gamma(t)$ during the relaxation to the ground state. All relaxation/conversion curves in this study have been measured similarly using the described approach.

SELF-DECELERATING RELAXATION: GENERAL TRENDS

We have investigated light-induced spin-state relaxation in neat compounds **I**–**III** at temperatures T = 5–16 K. At higher temperatures, the observed effect of light becomes very small, and relaxation to the ground state becomes fast for the studied compounds.

Figure 3 shows the relaxation curves for the compound **I** at T = 5, 10, and 13 K measured during 4 h after photoswitching.

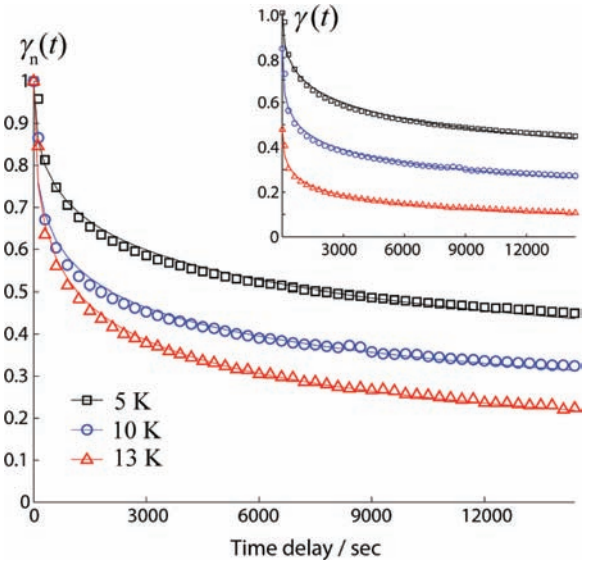

Figure 3. Normalized relaxation dependences $\gamma_n(t)$ for compound **I** measured at 5, 10, and 13 K (indicated in the legend). Solid lines show the simulations (parameters are given in Table 1). Inset: the same data shown for $\gamma(t)$ (before normalization).

Here and in most cases below, we plot the values $\gamma_n(t)$ normalized to the maximum of the conversion depth for the clarity of representation. Figure 4 compares $\gamma_n(t)$ dependences obtained at T = 5–16 K for compounds **I**–**III** measured during 1 h after photoswitching. Significant dependence of the relaxation rate is observed within this relatively narrow temperature range, and a noticeable difference between compounds is present. Remarkably, all of these curves demonstrate self-decelerating character of relaxation (most evident in Figure 3, relaxation data on a time scale of 4 h for compounds **II** and **III** is given in Figure S2 in the Supporting Information). They cannot be described by a monoexponential function; they also do not resemble self-accelerating sigmoidal curves.[35] The magnetic susceptibility dependence of compound **I** is characteristic of weak cooperativity (very gradual spin transition), whereas those of compounds **II** and **III** show strong cooperativity (abrupt spin transition). Therefore, regardless of the degree of cooperativity, breathing crystals demonstrate an unusual self-decelerating relaxation trend, opposite to the self-acceleration in neat iron(II) spin-crossover compounds.

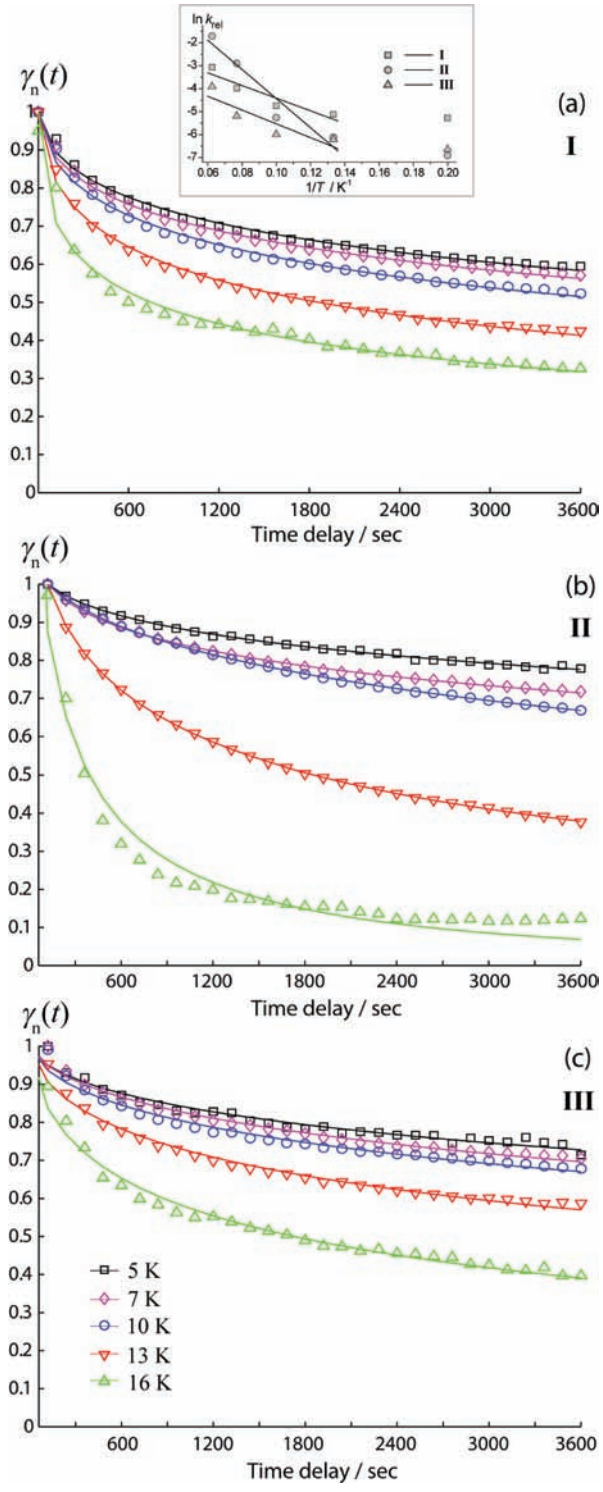

Figure 4. Normalized relaxation dependences $\gamma_n(t)$ measured for compounds **I**, **II**, and **III** (a, b, and c, respectively) at 5–16 K. Temperatures for all three compounds are indicated in the legend to panel c. Solid lines show the simulations (parameters are given in Table 1). Inset: pseudo-Arrhenius plot ln k_{rel} vs $1/T$.

Figures 3 and 4 allow for the following conclusions on general relaxation trends to be drawn: (i) the relaxation has a self-decelerating character for all three studied compounds; even at the lowest temperature (5 K), the shapes of the relaxation curves are pronouncedly self-decelerating; (ii) the relaxation rates vary noticeably from compound to compound;

dx.doi.org/10.1021/ic202248v | Inorg. Chem. 2012, 51, 709–717

and (iii) the relaxation rate increases drastically with temperature, and the character of this temperature dependence varies strongly from compound to compound. It is thus crucial to understand the origin of the self-decelerating behavior in breathing crystals and the main factors determining the dependences (ii) and (iii).

■ ORIGIN OF SELF-DECELERATING BEHAVIOR

The previous studies on spin-crossover compounds suggested two different explanations for the deviation of relaxation character from the monoexponential. In the first case, this was attributed to the dependence of the relaxation rate on the concentration of excited states.[35] This means that the characteristic parameter of exponential decay changes in time as the system relaxes to the ground state. This kind of explanation was used in the description of self-accelerating (sigmoidal) relaxation curves in a number of neat iron(II) spin-crossover compounds.[35] Another approach to describe the nonexponential relaxation in spin-crossover compounds was to assume that the relaxation rates are not equal for all excited states but are distributed in a certain range (usually described by a Gaussian).[35] As a result, the observed relaxation curve was in fact a convolution of monoexponentials corresponding to individual spin-crossover centers and having different characteristic decay times. In this way, a number of self-decelerating relaxation dependences were successfully described, including several cases of 1D iron(II) spin-crossover compounds.[35,38−41]

Considering excited-state relaxation in breathing crystals, the first approach (concentration dependence) can, in principle, explain self-deceleration assuming that the relaxation slows down as the number of excited states in the solid decreases. The second approach (distribution hypothesis) is also straightforward to explain self-deceleration, especially taking into account some conformational disorder found by X-ray for many breathing crystals.[11]

To distinguish between these two explanations, we have performed the experiments shown in Figure 5. Figure 5a shows the dependence of the conversion depth (i.e., the fraction of photoinduced WS state γ) on time for the same irradiation power but different repetition rate of the laser shots (10 and 5 Hz). First, the conversion curve is clearly not exponential (as to be expected from the Lambert−Beer law neglecting the bleaching). The initial rapid rise of the conversion during the first several minutes is followed by the long and slow tail, so that the plateau is not completely reached even after 40 min of illumination. The main factors explaining such behavior are the bleaching of the photoinduced WS state and competition of the photoexcitation with relaxation.[38,42] The crystals in the WS state are slightly more transparent as compared to the SS state; therefore, the bleaching effect is certainly present; however, the relaxation contribution is much more evident. Experiments with two repetition rates of the laser shots are different in two respects. First, the mean light power absorbed by the sample is by a factor of 2 larger for illumination with 10 Hz frequency. Second, the relaxation between laser shots should be less efficient for illumination with 10 Hz frequency (0.1 s for 10 Hz as compared to 0.2 s for 5 Hz frequency). The shapes of the conversion curves measured at 10 and 5 Hz are very close, but the values at the plateau reached at ca. 40 min are clearly different. This means that the relaxation significantly contributes during the time delays between the laser shots, and indeed, the larger fraction of WS states relaxes during illumination with 5 Hz. Thus, the extent of self-deceleration is

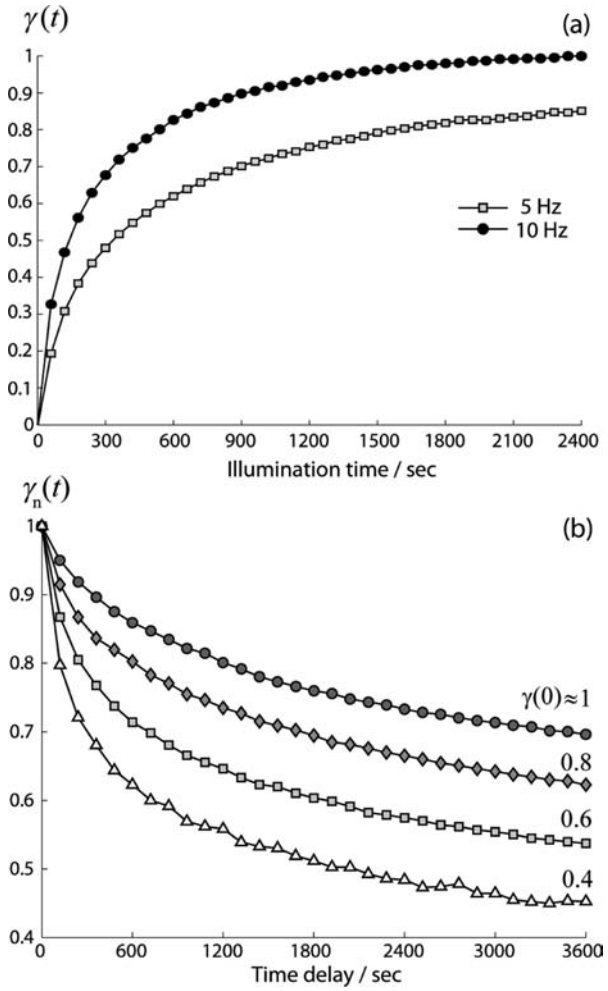

Figure 5. (a) Conversion depth vs illumination time measured for compound **I** at 5 K using two frequencies of laser shots (5 and 10 Hz as indicated in the legend). (b) Normalized relaxation dependences $\gamma_n(t)$ measured for compound **I** after illumination of different duration [initial conversion depth $\gamma(t = 0)$ is indicated on the right].

even larger as can be seen from Figures 3 and 4 where the beginning of the relaxation curve on subminute scale is not recorded.

Figure 5b shows the dependence of the relaxation on the initial conversion depth. The illumination time was varied to produce different initial concentration of photoinduced excited states (conversion depth ranging from ca. 0.4 to 1). It is clear that the relaxation rate does depend on the duration of photoexcitation. If the observed relaxation would be slower at lower initial concentration of excited states, self-deceleration could be explained by a concentration dependence of relaxation rate. However, the other way around, the relaxation is faster for smaller initial concentrations of the excited states. Thus, the first hypothesis discussed above (concentration dependence) can reliably be ruled out, and the distribution model is to be considered as the main explanation. On the other hand, the results of Figure 5b naturally lead to the conclusion that if the relaxation is faster at the low concentration of excited states, the observed relaxation should have taken the form of self-accelerating curve. Thus, the observed decrease of the relaxation rate for higher initial $\gamma(0)$ seems to contradict the self-decelerating shape of the relaxation curves and requires further explanation.

dx.doi.org/10.1021/ic202248v | Inorg. Chem. 2012, 51, 709−717

The results of Figure 5a show that a noticeable fraction (ca. 20%) of the excited states relaxes on the subsecond time scale; at the same time, as is evident from Figures 3 and 4, a larger fraction of the excited states relaxes on the time scale of hours. This means that the distribution of relaxation rates is very broad. It seems that the only way to explain the results of Figure 5b is to assume that the fraction of *fast-relaxing* clusters is excited already at *short* illumination times, whereas the fraction of *slow-relaxing* clusters is photoswitched only after *longer* illumination. This also agrees well with the shape of the conversion curves shown in Figure 5a that have the quite steep rise in the beginning (easily switchable fraction) followed by a much slower tail (hard-switchable fraction) approaching the maximum conversion value.

In principle, it is reasonable to expect that the easily switchable clusters are faster relaxing (whereas hard-switchable clusters are slower relaxing). The extinction coefficient for a crystal solid is very high (as was mentioned above); therefore, all light is absorbed on the size of the microcrystal following Lambert–Beer exponential law that introduces the gradient of concentrations along the direction of light. At the same time, the noticeable bleaching occurs in breathing crystals, since the optical density of the high-temperature state is smaller (although still very high) as compared to the low-temperature state. Thus, it is reasonable to expect that at short illumination times all light is absorbed in the thin layer close to the surface of the crystals, whereas the longer illumination results in the penetration of light deeper into the crystals. Considering the relaxation dependence shown in Figure 5b, it is reasonable to assume that the easily switchable fast-relaxing clusters are located in the near-surface layer, whereas the hard-switchable slow-relaxing clusters are located deeper in the crystal volume. Taking into account that the increase of the unit cell volume during the conversion from SS to WS state reaches ca. 13%, it is possible that the clusters located in the deeper layers experience stronger sterical hindrance for the conversion as compared to those located on the surface.

Alternatively, the distribution of photoswitching and relaxation characteristics in exchange-coupled clusters can be explained by some conformational disorder, regardless of the location with respect to the crystal surface. X-ray analysis shows that at high temperatures (WS state) orientations of the solvent molecules and alkyl substituents in nitroxides are disordered (as shown for propyl-benzene molecules in Figure 1).[11] Therefore, in principle, the conformational disorder can also be the reason for the broad distribution of the relaxation rates. Previously, the conformational disorder was introduced as the main factor responsible for the self-decelerating relaxation observed in 1D iron(II)-based spin-crossover compounds.[38]

The dependence of the photoswitching and relaxation on temperature can also be reasonably explained by the distribution of the relaxation rates in the sample (Figure 6). The maximum conversion depth measured during the illumination strongly depends on the temperature between 5 and 20 K (Figure 6a). This can be explained by electron relaxation competing with the formation of the WS state, so that the photoswitching itself becomes less efficient with an increase in the temperature. Alternatively, this can be explained by very fast relaxation from the WS to the SS state in some fraction of clusters (similar to Figure 5a), which grows in amount with the temperature.

The experiment shown in Figure 6b allows one to distinguish between these two explanations. We have performed photo-

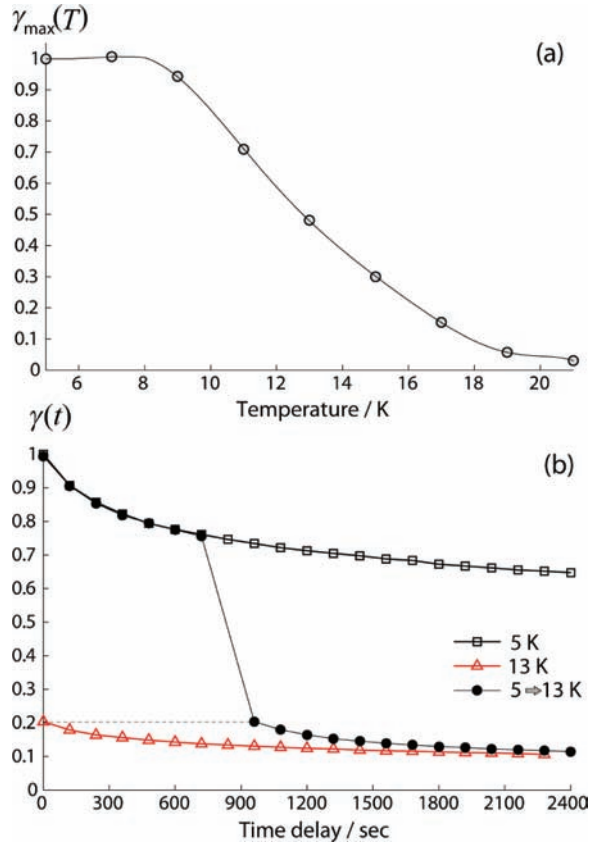

Figure 6. (a) Maximum (detectable) conversion depth for compound **I** vs temperature. (b) Relaxation dependences $\gamma(t)$ measured for compound **I** at 5 and 13 K, and experiment with a temperature change: The photoinduced WS state was prepared at 5 K and allowed to relax for 12 min at 5 K, and then, the temperature was changed to 13 K. Relaxation curves are normalized to $\gamma(t = 0)$ at 5 K. The dashed line indicates the level $\gamma(t = 0)$ at 13 K.

switching at T = 5 K to reach a maximum conversion depth to WS state; then, after 12 min of relaxation, the temperature was increased to 13 K (the estimated time of the temperature change and stabilization was 3–5 min). It is evident that some fraction of WS states relaxed rapidly during the temperature change. The conversion depth right after the temperature change nicely corresponds to the initial conversion (at t = 0) when photoswitching is performed at 13 K. At longer time delays after the temperature change, the relaxation curve gradually approaches the relaxation curve measured at 13 K. These observations confirm that (i) there is a distribution of relaxation rates in clusters photoswitched to WS state and (ii) the dependence of the maximum conversion depth on temperature is mainly due to the fast relaxation in some fraction (temperature-dependent) of the photoinduced WS states. Thus, the principal origin of the self-decelerating character of relaxation in breathing crystals is the distribution of the relaxation rates in photoinduced spin states.

■ MODELING OF SELF-DECELERATING RELAXATION

The simultaneous presence of clusters relaxing very fast (τ_{rel} < 1 min) and very slow (τ_{rel} > 1 h) implies that both quantum tunneling and thermally activated relaxation processes have to be considered. As was outlined in ref 35, in any case, thermally activated relaxation has to be considered as the tunneling from thermally excited levels. Thus, the relaxation rate constant of

dx.doi.org/10.1021/ic202248v | *Inorg. Chem.* 2012, 51, 709–717

Table 1. Parameters Obtained from the Simulation and Analysis of Relaxation Dependences $\gamma_n(t)$ Shown in Figures 3 and 4

			σ (cm^{-1})				
compd	k^0_{therm} (s^{-1})	E_A (cm^{-1})	T = 5 K	T = 7 K	T = 10 K	T = 13 K	T = 16 K
I	$(3.2 \pm 1.3) \times 10^{-3}$	19 ± 5	10.3	15.8	19.8	24.2	35.7
II	$(1.1 \pm 0.7) \times 10^{-1}$	44 ± 9	12.9	18.3	16.3	22.4	21.2
III	$(1.3 \pm 0.5) \times 10^{-3}$	21 ± 7	10.2	14.7	20.5	25.4	27.4

particular cluster can be written as:

$$k_{rel} = k_{tunnel} + k^0_{therm} \exp(-E_A/kT) \quad (4)$$

where k_{tunnel} is the tunneling rate constant in the low-temperature limit, k^0_{therm} is the pre-exponential factor for thermally activated relaxation, and E_A is the apparent activation energy that is different for different clusters. The tunneling term k_{tunnel} can also describe the distribution of relaxation rates via the account of different vibration modes.[43] However, Figure 4 shows that thermally activated processes become dominant already at T > 7 K, and thus, the first term in eq 4 can for simplicity be neglected (this is also confirmed by simulations discussed below). It is rather difficult to predict the distribution of E_A values theoretically, but an order-of-magnitude estimate of its center and its width can be done using experimental Figure 6a (compound **I**). Assume that those clusters that rapidly relax in between the laser flashes (<0.1 s) correspond to the kT values closely equal to or larger than the barrier height. At T = 5−7 K, the barrier height is larger than kT for all clusters since $\gamma_{max}(T) \approx 1$ in this range, whereas at T > 20 K, the opposite extreme $\gamma_{max}(T) \approx 0$ is reached, and thus, the barrier height is smaller than kT for nearly all clusters. Therefore, the width of the distribution of activation energies can be estimated as the difference between these two plateaus of $\gamma_{max}(T)$ that gives $\delta E_A \sim 15$ K. The center of this distribution should approximately correspond to the $\gamma_{max}(T) \approx 0.5$, that is, 13 K. This means that the width of the E_A distribution can be comparable to or even larger than its central value. In addition, the simultaneous existence of clusters relaxing on the subsecond time scale (Figure 5a) and time scale of hours (Figures 3 and 4) also implies the very broad (5 orders of magnitude) distribution of relaxation rates. This means that, for example, at T = 5 K, the activation energy can be distributed over as wide as $\delta E_A = kT \ln(10^5) \approx 50$ K. Discussing the absolute widths, quite large values of ca. 20−30 cm^{-1} for the standard deviation parameter σ of a Gaussian distribution have been found previously in iron(II) 1D spin-crossover compounds.[41] For simplicity, we have also modeled the relaxation curves for breathing crystals using the Gaussians that allowed us to achieve satisfactory agreement using reasonable parameters. The experimental dependences $\gamma_n(t)$ were least-squares fitted using the expression $k^{observed}_{rel} = k_{rel} \exp(-\delta E_A/kT)$, where δE_A was normally distributed around zero with the standard deviation parameter σ, and the values k_{rel} and σ were varied. The spread of the σ values (see Table 1) is probably caused by the simplicity of the model used; it is the next theoretical challenge to develop the distribution models allowing for the better fit of both self-decelerating curves and their temperature dependence. Note that quite large (up to 9 cm^{-1}) spread of σ values was also found previously in iron(II) 1D spin-crossover compound exhibiting self-decelerating (or "stretched exponential") relaxation behavior.[41] The temperature dependences of k_{rel} were analyzed using the pseudo-Arrhenius plot (inset in Figure 4) to obtain the estimate values of activation energy E_A and pre-exponential factor k^0_{therm} for all three compounds (eq 4 and Table 1). At T > 7 K, the description using the Arrhenius law is reasonably good, whereas noticeable deviation from linearity at 5 K probably occurs because the tunneling relaxation rate k_{tunnel} becomes comparable with the thermally activated relaxation rate. A higher accuracy of the obtained parameters (especially k^0_{therm}) cannot be achieved because the experimental data can only be measured in a relatively narrow temperature range for the studied compounds.

The observed increase of the distribution width with temperature is not very large in absolute terms but has a systematic character. Consider the energy diagram shown in Figure 7. The height of the potential barrier from the WS to the SS state according to Figure 6a and Table 1 is ca. 20−40 cm^{-1}. A much smaller depth of the potential well of WS state as compared to the one of SS state follows from the thermal spin transition temperatures of 100−200 K and agrees qualitatively with the calculations of ref 44. The structure of energy levels is much more complicated in breathing crystals as compared to the iron(II) spin-crossover compounds because of the low-lying excited spin levels. Every spin triad has three multiplets (two doublets and one quartet) separated by exchange interaction.[11−14] Typical values of (ferromagnetic) exchange interaction in WS state (axial coordination of nitroxides) are estimated as $J \sim 10$ cm^{-1},[45] meaning that the energy difference

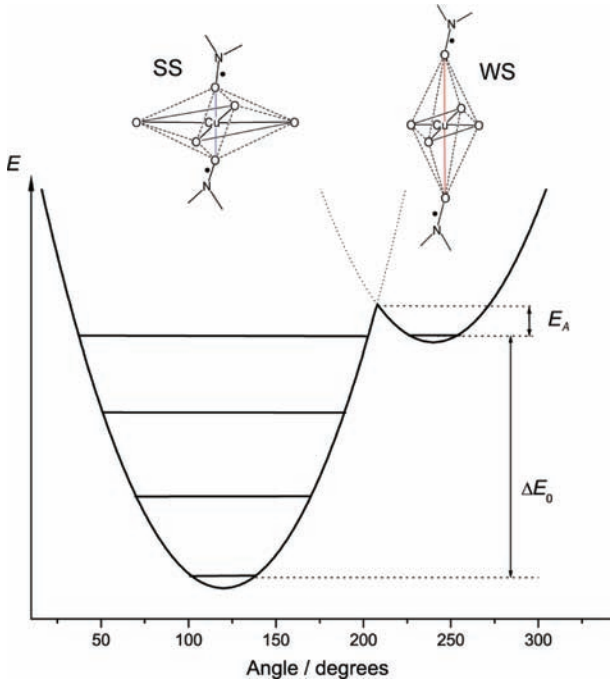

Figure 7. Schematic circular section of the potential energy surface associated with the two Jahn−Teller valleys in breathing crystals. Structures corresponding to SS and WS states are sketched on top. Spin levels of the triads are not shown for simplicity.

dx.doi.org/10.1021/ic202248v | Inorg. Chem. 2012, 51, 709−717

between the ground quartet and the upper doublet states equals to $3J \sim 30$ cm^{-1} (for spin-Hamiltonian written in a form $\hat{H}_{ex} = -2J\hat{S}_i\hat{S}_j$). This means that thermal population of the excited spin levels at $T = 5-16$ K cannot be neglected and that the tunneling can occur from these excited levels at elevated temperatures. In fact, the situation is even more complicated, since, as we have shown recently, the *intercluster* exchange interaction in breathing crystals (operating between polymer chains) is also of the order of 1−10 cm^{-1}.[19] This means that photoinduced WS states represent the exchange-coupled network where the magnitudes of inter- and intracluster exchange interactions are comparable. Thus, there is a number of the excited spin levels in WS state potential well between 0 and ca. 30 cm^{-1}, and thermal population of these levels leads effectively to the increase of the distribution width σ found in our simulations. In addition, there are of course excited levels corresponding to the E_g vibration mode of copper ($\hbar\omega \sim 300$ cm^{-1}[46−48]) lying significantly higher than the excited multiplets of spin triad of the ground vibrational state.

Note one more difference of the excited spin-state relaxation in breathing crystals and iron(II) spin-crossover compounds. In the case of iron(II), the tunneling rate depends on the spin−orbit coupling matrix element that makes the transition (relatively) weakly allowed.[35] In the case of breathing crystals, these relaxation transitions are allowed between the states of spin triad of the same multiplicity (doublets of WS state to doublet of SS state or similar quartet-to-quartet), and a large number of closely lying energy levels in photoinduced WS state makes these transitions efficient.

Finally, we compared semiquantitatively the relaxation trends in different compounds **I**−**III** of the breathing crystals family (Table 1 and Figure 4). In iron(II) spin-crossover compounds, the correlation between the temperature of thermal spin transition and the tunneling high-to-low spin state relaxation is well established.[35] In particular, the tunneling rate in the low-temperature limit should be faster for those compounds that exhibit thermal transitions at higher temperatures. In breathing crystals, a similar trend is expected. In principle, the tunneling rate in the low-temperature limit should correlate with the zero-point energy difference (see Figure 7) that in its turn correlates with the thermal spin transition temperature. However, as was shown above, the contribution of the thermally activated process is significant even at 5 K; therefore, it is rather difficult to obtain good estimates for the low-temperature tunneling rate and compare them in studied compounds. On the other hand, the height of the potential barrier E_A can be correlated with the temperature dependence of the excited spin-state relaxation. Compounds **II** and **III** exhibit abrupt spin transitions at significantly different temperatures; therefore, they fit well for the comparison of their relaxation behavior. Compound **II** exhibits a slightly slower relaxation at 5 K as compared to compound **III**; however, the relaxation in compound **II** speeds up more dramatically with temperature (Figure 4). This behavior is consistent with larger values k^0_{therm} and E_A in compound **II** as compared to compound **III** (Table 1). The depth of the WS state potential well (E_A) is expected to depend mainly on local geometry of CuO_6 octahedra. In our recent work, it was shown that among the other factors, the orientation of solvent molecule in WS/SS states strongly influences the character of magnetic anomaly.[11] Therefore, it is very reasonable to expect that the WS state potential depth is very sensitive to the subtle modifications of structure provided by inclusion of different solvent molecules in the interchain space. It is thus a target task to develop the compounds with higher E_A values allowing for LIESST-like manifestations at higher temperatures.

CONCLUSIONS AND OUTLOOK

In this work, we have studied the relaxation of the light-induced excited spin states in molecular magnets of "breathing crystals" family $Cu(hfac)_2L^R$. The observed relaxation occurs on a time scale of hours at cryogenic temperatures (<20 K) and has a pronounced self-decelerating character. This unusual trend is explained by a broad distribution of activation energies of relaxation in photoswitched exchange clusters. The broad distribution may originate from different sources. It is reasonable to expect that the clusters located closer to the surface of crystal relax faster, as structural rearrangements deep inside the crystal may be more sterically hindered as compared to the crystal surface. Alternatively, some conformational disorder in the crystal packing (orientations of solvent molecules and alkyl substituents of the nitroxides) was previously found by X-ray analysis. Finally, the existence of thermally populated low-lying spin levels of spin triads also gives rise to the distribution of the activation energies and thus relaxation parameters.

Remarkably, despite the crucial differences from iron(II) spin-crossover compounds, breathing crystals manifest many similarities such as the observation of thermal- and light-induced spin transitions, hysteresis loops, etc. In this work, we have found that the slow relaxation of the light-induced spin state in breathing crystals is also similar to the one observed for several iron(II) spin-crossover compounds in many respects. The broader distribution of electronic structure parameters in breathing crystals is not totally unexpected. First, these materials have principal 1D structure, which implies larger flexibility of polymer chains as compared to the 2D and 3D structures. Second, the changes of spin configuration in breathing crystals occur in the exchange-coupled cluster, not inside the d-shell of the spin-transition ion as is in iron(II) spin-crossover compounds. This principal difference allows one to expect that breathing crystals are much more sensitive to the *chemical* and *physical* external influences as compared to the iron(II) spin-crossover compounds. In perspective, this may be used for fine-tuning the properties of breathing crystals for various applications.

ASSOCIATED CONTENT

Supporting Information

Applicability of the spectroscopic approach used for quantification of conversion depth and relaxation and self-decelerating character of relaxation for compounds **II** and **III**. This material is available free of charge via the Internet at http://pubs.acs.org.

AUTHOR INFORMATION

Corresponding Author

*E-mail: mfedin@tomo.nsc.ru.

ACKNOWLEDGMENTS

This work was supported by the Russian Foundation for Basic Research (no. 11-03-00158), the RF President's Grant (MK-4268.2010.3), the Grant for the Leading Scientific Schools (NSh-7643.2010.3), and Federal Agency for Education (no. P 1144). We are very thankful to Dr. Sergey Veber (ITC-Novosibirsk) for technical assistance and stimulating dis-

cussions. We thank Alexander Semenov for participation in the early stages of this work.

REFERENCES

(1) Kahn, O. *Molecular Magnetism*; VCH: New York, 1993.
(2) *Molecular Magnetism: From Molecular Assemblies to the Devices (Nato ASI Series, E: Applied Sciences)*; Coronado, E., Delhaès, P., Gatteschi, D., Miller, J. S., Eds.; Kluwer Academic Publisher: Dordrecht, the Netherlands, 1996; Vol. *321*.
(3) *Spin Crossover in Transition Metal Compounds*; Gütlich, P., Goodwin, H. A., Eds.; Topics in Current Chemistry, 233−235; Springer-Verlag: Berlin, Heidelberg, NY, 2004; Vols. *I*−*III*.
(4) Decurtins, S.; Gutlich, P.; Kohler, C. P.; Spiering, H.; Hauser, A. *Chem. Phys. Lett.* **1984**, *105*, 1−4.
(5) Gutlich, P.; Hauser, A.; Spiering, H. *Angew. Chem., Int. Ed. Engl.* **1994**, *33*, 2024−2054.
(6) Sato, O. *Acc. Chem. Res.* **2003**, *36*, 692−700.
(7) Bousseksou, A.; Molnar, G.; Salmon, L.; Nicolazzi, W. *Chem. Soc. Rev.* **2011**, *40*, 3313−3335.
(8) Ovcharenko, V. I.; Fokin, S. V.; Romanenko, G. V.; Shvedenkov, Yu. G.; Ikorskii, V. N.; Tretyakov, E. V.; Vasilevskii, S. F. *J. Struct. Chem.* **2002**, *43*, 153−167.
(9) Ovcharenko, V. I.; Maryunina, K. Yu.; Fokin, S. V.; Tretyakov, E. V.; Romanenko, G. V.; Ikorskii, V. N. *Russ. Chem. Bull., Int. Ed* **2004**, *53*, 2406−2427.
(10) Ovcharenko, V. I.; Romanenko, G. V.; Maryunina, K. Yu.; Bogomyakov, A. S.; Gorelik, E. V. *Inorg. Chem.* **2008**, *47*, 9537−9552.
(11) Romanenko, G. V.; Maryunina, K. Yu.; Bogomyakov, A. S.; Sagdeev, R. Z.; Ovcharenko, V. I. *Inorg. Chem.* **2011**, *50*, 6597−6609.
(12) Fedin, M.; Veber, S.; Gromov, I.; Ovcharenko, V.; Sagdeev, R.; Schweiger, A.; Bagryanskaya, E. *J. Phys. Chem. A* **2006**, *110*, 2315−2317.
(13) Fedin, M.; Veber, S.; Gromov, I.; Ovcharenko, V.; Sagdeev, R.; Bagryanskaya, E. *J. Phys. Chem. A* **2007**, *111*, 4449−4455.
(14) Fedin, M.; Veber, S.; Gromov, I.; Maryunina, K.; Fokin, S.; Romanenko, G.; Sagdeev, R.; Ovcharenko, V.; Bagryanskaya, E. *Inorg. Chem.* **2007**, *46*, 11405−11415.
(15) Veber, S. L.; Fedin, M. V.; Potapov, A. I.; Maryunina, K. Yu.; Romanenko, G. V.; Sagdeev, R. Z.; Ovcharenko, V. I.; Goldfarb, D.; Bagryanskaya, E. G. *J. Am. Chem. Soc.* **2008**, *130*, 2444−2445.
(16) Veber, S. L.; Fedin, M. V.; Maryunina, K. Yu.; Romanenko, G. V.; Sagdeev, R. Z.; Bagryanskaya, E. G.; Ovcharenko, V. I. *Inorg. Chim. Acta* **2008**, *361*, 4148−4152.
(17) Fedin, M. V.; Veber, S. L.; Romanenko, G. V.; Ovcharenko, V. I.; Sagdeev, R. Z.; Klihm, G.; Reijerse, E.; Lubitz, W.; Bagryanskaya, E. G. *Phys. Chem. Chem. Phys.* **2009**, *11*, 6654−6663.
(18) Fedin, M. V.; Veber, S. L.; Sagdeev, R. Z.; Ovcharenko, V. I.; Bagryanskaya, E. G. *Russ. Chem. Bull., Int. Ed.* **2010**, *59*, 1065−1079.
(19) Fedin, M. V.; Veber, S. L.; Maryunina, K. Y.; Romanenko, G. V.; Suturina, E. A.; Gritsan, N. P.; Sagdeev, R. Z.; Ovcharenko, V. I.; Bagryanskaya, E. G. *J. Am. Chem. Soc* **2010**, *132*, 13886−13891.
(20) Veber, S. L.; Fedin, M. V.; Maryunina, K. Y.; Potapov, A.; Goldfarb, D.; Reijerse, E.; Lubitz, W.; Sagdeev, R. Z.; Ovcharenko, V. I.; Bagryanskaya, E. G. *Inorg. Chem.* **2011**, *50*, 10204−10212.
(21) Fedin, M.; Ovcharenko, V.; Sagdeev, R.; Reijerse, E.; Lubitz, W.; Bagryanskaya, E. *Angew. Chem., Int. Ed.* **2008**, *47*, 6897−6899; *Angew. Chem.* **2008**, *120*, 7003−7005.
(22) Matsumoto, S.; Higashiyama, T.; Akutsu, H.; Nakatsuji, S. *Angew. Chem.* **2011**, *50*, 10879−10883.
(23) Okazawa, A.; Ishida, T. *Inorg. Chem.* **2010**, *49*, 10144−10147.
(24) Setifi, F.; Benmansour, S.; Marchivie, M.; Dupouy, G.; Triki, S.; Sala-Pala, J.; Salaun, J.-Y.; Gomez-García, C. J.; Pillet, S.; Lecomte, C.; Ruiz, E. *Inorg. Chem.* **2009**, *48*, 1269−1271.
(25) Okazawa, A.; Hashizume, D.; Ishida, T. *J. Am. Chem. Soc.* **2010**, *132*, 11516−11524.
(26) Baskett, M.; Lahti, P. M.; Paduan-Filho, A.; Oliveira, N. F. *Inorg. Chem.* **2005**, *44*, 6725−6735.
(27) dePanthou, F. L.; Belorizky, E.; Calemczuk, R.; Luneau, D.; Marcenat, C.; Ressouche, E.; Turek, P.; Rey, P. *J. Am. Chem. Soc.* **1995**, *117*, 11247−11253.
(28) Caneschi, A.; Chiesi, P.; David, L.; Ferraro, F.; Gatteschi, D.; Sessoli, R. *Inorg. Chem.* **1993**, *32*, 1445−1453.
(29) Gütlich, P.; Poganiuch, P. *Angew. Chem.* **1991**, *103*, 1015−1017; *Angew. Chem., Int. Ed. Engl.* **1991**, *30*, 975−977.
(30) Hauser, A.; Jeftic, J.; Romstedt, H.; Hinek, R.; Spiering, H. *Coord. Chem. Rev.* **1999**, *190*−*192*, 471−491.
(31) Breuning, E.; Ruben, M.; Lehn, J.-M.; Renz, F.; Garcia, Y.; Ksenofontov, V.; Gütlich, P.; Wegelius, E.; Rissanen, K. *Angew. Chem.* **2000**, *112*, 2563−2566; *Angew. Chem., Int. Ed.* **2000**, *39*, 2504−2507.
(32) Renz, F.; Oshio, H.; Ksenofontov, V.; Waldeck, M.; Spiering, H.; Gütlich, P. *Angew. Chem.* **2000**, *112*, 3832−3834; *Angew. Chem., Int. Ed.* **2000**, *39*, 3699−3700.
(33) Bonhommeau, S.; Molnar, G.; Galet, A.; Zwick, A.; Real, J.-A.; McGarvey, J. J.; Bousseksou, A. *Angew. Chem.* **2005**, *117*, 4137−4141; *Angew. Chem., Int. Ed.* **2005**, *44*, 4069−4073.
(34) Sato, O.; Tao, J.; Zhang, Y.-Z. *Angew. Chem.* **2007**, *119*, 2200−2236; *Angew. Chem., Int. Ed.* **2007**, *46*, 2152−2187.
(35) Hauser, A. In *Topics in Current Chemistry*; Gütlich, P., Goodwin, H. A., Eds.; Springer-Verlag: Berlin, Heidelberg, 2004; Vol. *234*, pp 155−198.
(36) Hauser, A.; Adler, J.; Gutlich, P. *Chem. Phys. Lett.* **1988**, *152*, 468−472.
(37) Stoll, S.; Schweiger, A. *J. Magn. Reson.* **2006**, *178*, 42−55.
(38) Mishra, V.; Mishra, H.; Mukherjee, R.; Codjovi, E.; Linares, J.; Letard, J.-F.; Desplanches, C.; Balde, C.; Enachescu, C.; Varret, F. *Dalton Trans.* **2009**, 7462−7472.
(39) Enachescu, C.; Linares, J.; Varret, F.; Boukheddaden, K.; Codjovi, E.; Salunke, S. G.; Mukherjee, R. *Inorg. Chem.* **2004**, *43*, 4880−4888.
(40) Neville, S. M.; Leita, B. A.; Halder, G. J.; Kepert, C. J.; Moubaraki, B.; Letard, J.-F.; Murray, K. S. *Chem.—Eur. J.* **2008**, *14*, 10123−10133.
(41) Dupouy, G.; Triki, S.; Marchivie, M.; Cosquer, N.; Gomez-Garcia, C. J.; Pillet, S.; Bendeif, E.-E.; Lecomte, C.; Asthana, S.; Letard, J.-F. *Inorg. Chem.* **2010**, *49*, 9358−9368.
(42) Enachescu, C.; Stoleriu, L.; Stancu, A.; Hauser, A. *Phys. Rev. B* **2010**, *82*, 104114.
(43) Bonhommeau, S.; Brefuel, N.; Palfi, V. K.; Molnar, G.; Zwick, A.; Salmon, L.; Tuchagues, J.-P.; Sanchez Costa, J.; Letard, J.-F.; Paulsen, H.; Bousseksou, A. *Phys. Chem. Chem. Phys.* **2005**, *7*, 2909−2914.
(44) Vancoillie, S.; Rulisek, L.; Neese, F.; Pierloot, K. *J. Phys. Chem. A* **2009**, *113*, 6149−6157.
(45) Allao, R.; Jordao, A.; Resende, J.; Cunha, A.; Ferreira, V.; Novak, M.; Sangregorio, C.; Sorace, L.; Vaz, M. *Dalton Trans.* **2011**, *40*, 10843−10850.
(46) Riley, M. J.; Hitchman, M. A.; wan Mohammed, A. *J. Chem. Phys.* **1987**, *87*, 3766−3778.
(47) Simmons, C. J.; Stratemeier, H.; Hanson, G. R.; Hitchman, M. A. *Inorg. Chem.* **2005**, *44*, 2753−2760.
(48) Hitchman, M. A.; Maaskant, W.; van der Plas, J.; Simmons, C. J.; Stratemeier, H. *J. Am. Chem. Soc.* **1999**, *121*, 1488−1501.